Electrical Power and Energy Systems 121 (2020) 106045

Contents lists available at ScienceDirect

Electrical Power and Energy Systems

journal homepage: www.elsevier.com/locate/ijepes

Evaluation of bi-directional cascading failure propagation in integrated electricity-natural gas system☆

Zhejing Bao[a], Zhewei Jiang[a], Lei Wu[b,*]

[a] College of Electrical Engineering, Zhejiang University, Hangzhou 310027, China
[b] Department of Electrical and Computer Engineering, Stevens Institute of Technology, NJ 07901 USA

ARTICLE INFO

Keywords:
Cascading failure
Dynamic gas transmission
Integrated electricity–natural gas system
Steady-state power flow
Evaluation

ABSTRACT

This paper aims at evaluating the bi-directional cascading failure propagation in integrated electricity-natural gas system (IEGS), with energy coupling components such as gas-fired generators and electricity-driven gas compressors. An integrated simulation approach is proposed to describe cascading failure propagation resulting from various triggering events, in which steady-state power flow, dynamic gas transmission, and working mode switching of gas compressors are considered. Electricity network islanding, re-dispatching of electricity generation and gas source pressure, as well as electricity and gas load shedding simulate the consequence of interactive cascading failure propagation. When a new steady state of IEGS is reached after the occurrence of an initial failure in either electricity or gas sub-system, the statistical indices with respect to energy supply availability of IEGS are calculated to assess risks caused by the cascading failure, and significances of individual electricity branches and gas pipelines are evaluated. An IEGS, consisting of a 24-bus 35-branch electricity grid and a 28-node 25-branch gas network coupled by two electricity-driven gas compressors and three gas-fired generators, is established to validate the proposed approach. Numerical simulations illustrate distinct characteristics of electricity and gas sub-systems in the cascading failure propagation process as well as different impacts of each sub-system on the other.

1. Introduction

The integrated electricity-natural gas system (IEGS) is becoming a focus of research and application, due to public awareness and policy incentives on fossil fuel depletion, climate change, and environmental pollution issues [1,2]. In an IEGS, electricity and natural gas sub-systems are interconnected as a unified system by energy coupling components, such as electricity-driven gas compressors and gas-fired electricity generators [3–5]. The increasing interdependence between electricity and natural gas sub-systems induced by the growing number of energy coupling components has brought significant attentions to the issues related to the gas-electric interface coordination, the strategic behavior in coupled energy markets, the coordinated market mechanism, and the regulatory environment [6–8].

The complicated interactions between the electricity and natural gas sub-systems impose significant challenges on the reliable operation of IEGS [9,10]. Indeed, a failure or disruption triggered in one sub-system could propagate to the other through energy coupling components, and, consequently affect operation of various facilities in IEGS. Even worse, the propagation of failure might reflect back to the triggering sub-system and induce even more severe failures [11]. For instance, under extreme weather or operation conditions, power transmission lines may encounter outages, which would lead to adjustments of generations and/or loads and further induce forced outage of electricity-driven compressors; the latter case could cause inlet pressures of gas-fired generators lower than the threshold, which would force the generators offline and induce a more disastrous disruption in the electricity network. Consequently, a dynamic model to accurately describe the aforementioned cascading failure propagation process in IEGS and a failure propagation evaluation approach are in urgent need for the reliable operation of IEGS, which would help IEGS operators secure the most important electricity branches, gas pipelines, and gas sources to avoid potential catastrophic disasters.

The interdependence between electricity generation sub-system and natural gas sub-system as well as the implications for energy security have attracted wide attention [12,13]. The short-term interdependence

☆ The National Natural Science Foundation of China under Grant no. 51777182, and in part supported by the U.S. National Science Foundation under Grant no. CMMI-1635339.

* Corresponding author at: ECE Department, Stevens Institute of Technology, Hoboken, NJ 07030, USA.
E-mail address: lei.wu@stevens.edu (L. Wu).

https://doi.org/10.1016/j.ijepes.2020.106045
Received 29 August 2019; Received in revised form 20 March 2020; Accepted 25 March 2020
Available online 20 April 2020
0142-0615/

of the two infrastructures was analyzed in [10,14–18]. The impact of natural gas infrastructure contingencies on the operation of electric power systems was studied in [10]. The impact of natural gas system operation on the short-term security of power system was assessed in [14] with a simplified gas network, while more accurate natural gas flow models were considered in [15] and [16]. An integrated simulation model was introduced in [17] to reflect the system dynamics in case of disruptions, by modelling electricity and gas systems separately while considering their linkages via an interface. A novel quasi-dynamic simulation model was proposed and implemented in the simulation tool *SAInt* (Scenario Analysis Interface for Energy Systems) to analyze the bidirectional interconnection between the two energy systems and the impact of various contingencies on secure supply of IEGS [18]. The simulation framework [19], consisting of a transient model for gas system and a steady state model for power system, was implemented into *SAInt* to perform a contingency analysis for a real world example. Convex optimization based steady state and transient simulation for IEGS was developed in [20] to provide practical results by correctly capturing the time evolution of line pack, while also investigating the impacts of wind power forecast errors on gas-network operations. The interval methods for uncertainty analysis were presented in [21] to study the impact of wind power on the steady-state operation of IEGS, as compared to the Monte Carlo simulation methods.

The impacts of interdependence on midterm coordinated scheduling and integrated long-term planning of IEGS were discussed in [22–35]. A two-stage mixed-integer linear stochastic optimization model was developed to analyze the electricity generation scheduling under gas supply uncertainty [22]. A planning approach has been proposed to reduce the impacts that failure events in natural gas network could impose on the electricity market operation [23]. In order to consider uncertainties in gas and electricity demand growth, a two-stage stochastic optimization was formulated to achieve coordinated expansion planning in IEGS [24]. A two-stage robust model was proposed to resolve day-ahead coordinated scheduling of IEGS with electricity and gas uncertainties [25]. A robust co-optimization planning model including a joint N-1 and probabilistic reliability criterion was introduced to promote economical and reliable planning of IEGS [26]. A security-constrained optimal power and gas flow of IEGS, formulated as a mixed-integer linear programming (MILP) problem, was proposed in [27]. A probabilistic energy flow framework of IEGS was studied while considering correlated varying energy demands and wind power [28]. A novel integrated model was introduced in [29] with a special focus on accurately simulating interdependences between the two networks in the presence of P2G. An integral formulation for steady-state analysis of IEGS was studied in [30], considering temperature dynamics in gas system operation and primary frequency regulation in electricity system. The coordinated scheduling of IEGS was described as a bi-level programming formulation from the independent system operator's viewpoint in [31]. A robust defense strategy for IEGS against malicious attacks was formulated as a tri-level optimization problem in [32]. Stochastic security-constrained scheduling of coordinated electricity and natural gas infrastructures was investigated in [33]. A tri-level robust optimization based network hardening model for enhancing resilience of IEGS against natural disasters was developed in [34]. A distributionally robust scheduling model for IGES was developed in [35] while considering integrated gas-electricity demand response.

The quantitative analysis for the impacts of cascades on reliable energy service of IEGS has been researched in [36–38]. With the statistical approaches, such as central moment [36] and multidimensional normal integral [37], some innovative research has been implemented on the failure probability estimation of gas supply in an IEGS, considering the correlation among the uncertainties such as intermittent wind power as well as stochastic heating demands and gas deliverability. Structural vulnerability assessment of multi-energy system has been studied using a PageRank algorithm [38], in which the importance of topological structure and static energy flow are included. These researches either represent a statistical analysis or employ a static approach, without elaborately simulating the interactive process during the cascades while considering the important coupling component such as electricity-driven natural gas compressor.

In order to bridge the gap, for the IEGS with energy coupling components, such as gas-fired generators and electricity-driven gas compressors, this paper develops a simulation and evaluation approach to studying the cascading failures propagation process between the electricity and gas systems and its impacts on the reliable energy service of IEGS. Moreover, with this approach, critical components in IEGS can be identified, which, if out of service, can lead to significant losses of electricity and/or gas service. The main contributions are summarized as follows:

1. An integrated co-simulation approach is developed to describe the cascading failure propagation process in IEGS, while considering steady-state DC power flow and dynamic gas transmission. Electricity network islanding as well as dispatching of electricity generation and gas source pressure, electricity/gas load shedding are also considered, triggered by branch outages, insufficient energy supplies, and gas pressure violations.
2. Based on the co-simulation of failure spreading process, quantitative evaluation approach to the consequence of cascading failures in IEGS is introduced, which can help identify the critical electricity branches and gas pipelines. Statistical analysis of evaluation indexes can discover the distinctive characteristics of electricity and gas subsystems showing in cascading process and the different cascading influence of each sub-system on the other.

The remaining of this paper is organized as follows. The integrated co-simulation and evaluation approach for cascading failures in IEGS is described in Section 2. Simulation results and discussions are given in Section 3. The conclusions are drawn in Section 4.

2. Integrated co-simulation and evaluation approach for cascading failures in IEGS

2.1 Integrated co-simulation framework

Transportation of electricity and natural gas occurs at different timescales, from milliseconds to hours. Specifically, electric energy travels at the speed of light, while the velocity of natural gas delivery is typically as low as 10 m/s [18]. To this end, a disturbance or failure could drive the electricity system reaching to a new operation state instantaneously. On the contrary, in natural gas system a disturbance or failure can lead to a non-negligible transient process before reaching to a new steady state. Consequently, in the co-simulation of cascading failures in IEGS, in order to accurately represent significantly different characteristics, the steady-state model of electricity power flow is considered while the dynamic model of natural gas transmission is applied.

The proposed integrated co-simulation approach is illustrated in Fig. 1 to describe the failure propagation in IEGS. DC power flow model based electric energy dispatch, including electricity network islands formation, generation adjustment, and load shedding, is implemented every ΔT. While during the time period between two consecutive electricity dispatching runs, the natural gas dispatching is conducted considering dynamic natural gas flow with a much shorter simulation step Δt, where the gas source pressure adjustment and gas load shedding are implemented. After the electricity dispatching, natural gas consumptions of gas-fired generators and the on/off states of compressors are transmitted to the gas dispatching. Similarly, the electricity demands consumed by compressors and the on/off states of gas-fired generators derived from the gas dispatching are passed to the following electricity dispatching. The alternating execution of electricity and natural dispatching, along with the exchange of values of energy

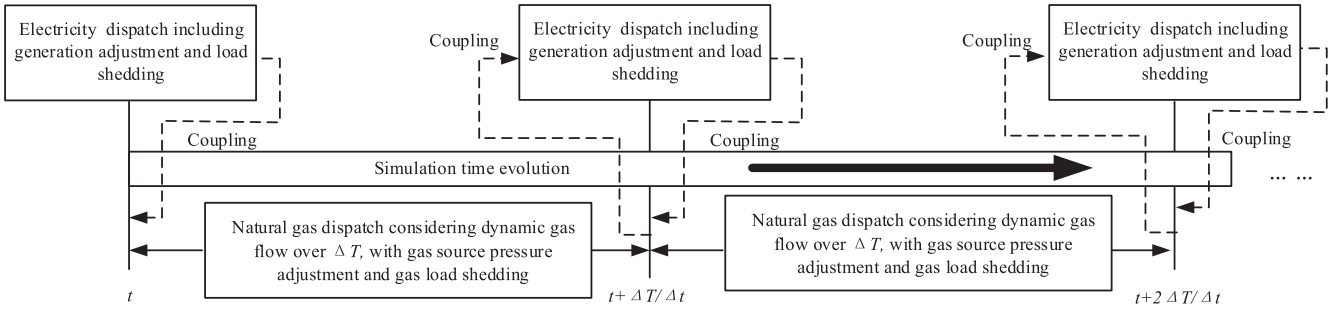

Fig. 1. Schematic diagram of the integrated co-simulation framework for cascading failures in IEGS.

coupling variables between them, carries over the entire evolution process, which constitutes an integrated co-simulation solution to discover the cascading failure propagation process in IEGS. It is worthwhile to mention that, during the gas dispatching over ΔT, if significant operating variation of gas compressors or gas-fired generators occurs because of the violation of physical constraints, the electricity dispatch will be triggered immediately instead of waiting for the next ΔT.

2.2 Linkage between electrical and gas networks

In the IEGS, the electricity and natural gas sub-systems are coupled by two types of coupling components, i.e., gas-fired generators and electricity-driven gas compressors. A gas-fired generator acts as a source in electricity network and a load in gas network, while an electricity-driven natural gas compressor works on the opposite way.

A gas-fired generator links the gas and electricity sub-systems by consuming natural gas to generate electricity, which can be modeled as

$$M_{g2p}(t) = \alpha P_{g2p}(t) \tag{1}$$

where $M_{g2p}(t)$ (kg/s) is the mass flow rate of gas consumption, $P_{g2p}(t)$ is the electricity power generation, parameters α is energy conversion coefficients. In natural gas transmission, gas flows in pipelines will face with pressure drop due to frictional resistance. Thus, natural gas compressors are installed along pipelines, in order to maintain pressures when delivering the natural gas from gas sources to end customers. The compressors are usually driven by natural gas or electricity, while the wide deployment of electricity-driven compressor would further intensify the interdependence between the electricity and gas systems. To this end, in this work, electricity-driven natural gas compressor is considered. The electricity power consumption $P_{com}(t)$ of a compressor for boosting the mass flow $M_{com}(t)$ from the inlet pressure $p_{in}(t)$ to outlet pressure $p_{out}(t)$ can be described by the following expression [15]

$$P_{com}(t) = f\frac{k}{k-1}\frac{RTZ\rho_n}{K_1}M_{com}(t)\left[\left(\frac{p_{out}(t)}{p_{in}(t)}\right)^{\frac{k-1}{k}} - 1\right] \tag{2}$$

where f is a factor denoting the fraction of total driving electric power provided by electric drivers, and others are empirical parameters of compressors. Eq. (2) indicates that the electric power consumption of compressor is positively related to the mass flow rate it carries as well as the pressure ratio between suction and discharge.

For a compressor, the mass flow rate it carries, the pressure ratio, and the gas pressure at outlet are constrained by their corresponding operation limits

$$M_{com}^{min} \leqslant M_{com}(t) \leqslant M_{com}^{max} \tag{3}$$

$$PR_{min} \leqslant \frac{p_{out}(t)}{p_{in}(t)} \leqslant PR_{max} \tag{4}$$

$$p_{out}^{min} \leqslant p_{out}(t) \leqslant p_{out}^{max} \tag{5}$$

Usually, a natural gas compressor can operate in the following four modes:

(1). Mode 1 with a fixed mass flow rate: In the normal operation, a compressor usually works in this mode, with the fixed mass flow rate limited by constraint (3).
(2). Mode 2 with a fixed boost ratio: The pressure ratio of a compressor can rise or drop by a disturbance or failure. When the pressure ratio reaches its upper or lower bounds, this operation mode may be triggered.
(3). Mode 3 with a fixed outlet pressure: The upper or lower limit of the outlet pressure can be reached during the cascading failure and then this work mode will be activated.
(4). Mode 4 with pressure ratio being 1: This mode is triggered when the compressing function fails, for example, caused by the loss of electricity supply.

2.3 Natural gas dispatching considering dynamic gas flow

Unlike the electricity network, it would take a much longer time for the natural gas network to reach a new steady state after a disturbance or failure. To describe such transmission characteristics, the dynamic model of the gas network is applied in this study [39]. In the next, we take period $[t, t + \Delta T/\Delta t]$ shown in Fig. 1 as an example to illustrate the natural gas dispatching while considering dynamic gas flow.

Natural gas transmission through pipelines is governed by the basic principles of fluid dynamics, including the material-balance equation and the momentum equation, namely Navier-Stokes equation. These are partial differential equations, relating mass flow rates and pressures with time and position along pipeline. With the Wendroff difference method, partial differential equations can be reformulated as

$$\begin{aligned} &p_n(t+l+1) + p_m(t+l+1) - p_n(t+l) - p_m(t+l) \\ &+ \frac{\Delta t \cdot c^2}{L_{mn}A_{mn}}[M_n(t+l+1) - M_m(t+l+1) + M_n(t+l) - M_m(t+l)] \\ &= 0,\ l = 0,\cdots,Ns-1 \end{aligned} \tag{6}$$

$$\begin{aligned} &\frac{1}{A_{mn}}(M_n(t+l+1) + M_m(t+l+1) - M_n(t+l) - M_m(t+l)) \\ &+ \frac{\Delta t}{L_{mn}}[p_n(t+l+1) - p_m(t+l+1) + p_n(t+l) - p_m(t+l)] \\ &+ \frac{\lambda \Delta t \varpi_{mn}}{4d_{mn}A_{mn}}(M_n(t+l+1) + M_m(t+l+1) + M_n(t+l) + M_m(t+l)) \\ &= 0,\ l = 0,\cdots,Ns-1 \end{aligned} \tag{7}$$

where $Ns = \Delta T/\Delta t$ denoting the number of gas dynamics simulations between two consecutive electricity dispatch calculations. ϖ_{mn} is the average gas flow rate in m/s and can be calculated as $\varpi_{mn} = \frac{c^2}{2A_{mn}}\left(\frac{M_m(t)}{p_m(t)} + \frac{M_n(t)}{p_n(t)}\right)$.

In addition to the flow equations, in natural gas network, the boundary conditions are also considered at intersections where nodes m, $m+1$, $m+2$,… are connected, which can be modeled as follows

$$p_m(t+l+1) = p_{m+1}(t+l+1) = p_{m+2}(t+l+1) = \cdots, l = 0, \cdots, Ns-1 \tag{8}$$

$$M_m(t+l+1) + M_{m+1}(t+l+1) + M_{m+2}(t+l+1) + \cdots = 0,\ l = 0, \cdots, Ns-1 \tag{9}$$

In gas network, generation and non-generation gas loads are susceptible to pressure losses. If pressure constraint (10) at gas node m is violated, gas load at node m will be shed automatically. Similarly, gas load shedding induced by violations of mass flow rate constraints can also be considered. However, in actual natural gas transmission system, this situation rarely occurs and is not considered in this paper.

$$p_m^{\min} \leqslant p_m(t+l+1) \leqslant p_m^{\max},\ l = 0, \cdots, Ns-1 \tag{10}$$

Two strategies of natural gas dispatching are implemented as follows. In Strategy I, considering the slow dynamics and limited monitoring in the gas network unlike the electric network, gas source and load nodes still work at their CP-VR (constant pressure and variable mass flow rate) and CR-VP (constant mass flow rate and variable pressure) modes, respectively, i.e., the pressures at gas source nodes and the mass flow rates at gas load nodes are kept constant during the time span of one gas dynamics simulation, i.e.,

$$p_m(t+l+1) = const,\ l = 0, \cdots, Ns-1,\ m \in S_{\mathrm{GS}} \tag{11}$$

where S_{GS} is the set of gas source nodes.

$$M_n(t+l+1) = const,\ l = 0, \cdots, Ns-1,\ n \in S_{\mathrm{GD}} \tag{12}$$

where S_{GD} is the set of gas load nodes.

In Strategy II, the pressures at gas source nodes and the mass flow rates at gas demand nodes are optimized while ensuring operational constraints in the gas network. The optimization objective is chosen as in (13),

$$\min \sum_{l=0}^{Ns-1} \sum_{j \in S_{\mathrm{GS}}} cp_j(t+l+1)(\Delta\bar{p}_j(t+l+1) + \Delta\underline{p}_j(t+l+1)) + \sum_{i \in S_{\mathrm{GD}}} cg_i(t)(M_i^0 - M_i(t+l+1)) \tag{13}$$

where M_i^0 is the initial gas mass flow rate at node i, the cost coefficients $cg_i(t)$ for gas demand shedding are higher than $cp_j(t)$ for gas source pressure adjustment. This is consistent with the fact that a higher priority is given to dispatching gas source pressures than shedding gas demands when failure occurs.

In (13), the upward and downward adjustments $\Delta\bar{p}_j(t+l+1)$and $\Delta\underline{p}_j(t+l+1)$of gas source pressure shall satisfy the following constraints:

$$0 \leqslant \Delta\bar{p}_j(t+l+1) \leqslant \bar{I}_j(t+l+1)(p_j^{\max} - p_j(t)) \tag{14}$$

$$0 \leqslant \Delta\underline{p}_j(t+l+1) \leqslant \underline{I}_j(t+l+1)(-p_j^{\min} + p_j(t)) \tag{15}$$

The two binary variables $\bar{I}_j(t+l+1)$ and $\underline{I}_j(t+l+1)$ are introduced to represent the upward or downward directions of gas source pressure adjustments. They shall satisfy:

$$\bar{I}_j(t+l+1) + \underline{I}_j(t+l+1) = 1 \tag{16}$$

In Strategy II, the objective (13) and the constraints (6)-(10), (14)-(16) constitute a MILP problem, which can be solved by Cplex. In Strategy I, the dynamic natural gas model (6)-(12) constitutes a LP problem, in which the number of unknown decision variables is equal to that of constraints. Take $Ns = 1$ as an example. For the pipeline mn, the decision variables include 4 continuous variables, $p_n(t+1)$, $p_m(t+1)$, $M_n(t+1)$, and $M_n(t+1)$, describing the pressures and mass flow rates at two ending nodes m and n. Thus, for the gas network with L pipelines, $4L$ decision variables will be solved. The number of constraints in Eqs. (6) and (7) is $2L$. The numbers of intersection and non-intersection nodes are assumed to be N_{cross} and $N_{\mathrm{non\text{-}cross}}$, and the number of nodes directly connected with the intersection node i is called the degree, denoted as Deg_i. The numbers of constraints (8) and (9) for intersection node i is equal to Deg_i, and the number of constraints (11) and (12) for the pressures and mass flow rates of non-intersection node j is Deg_j. The sum of Deg_i and Deg_j is $2L$. Consequently, Strategy I is a LP problem with the same numbers of decision variables and constraints. By solving these LP problems, pressures and mass flow rates at two ending nodes m and n of a gas pipeline can be determined.

2.4 Electricity dispatch

When outages of electricity branches and/or gas-fired generators, or/and the electricity consumption variation of gas compressors arise, the electricity dispatch problem is implemented for the electricity network. If the entire grid is separated into several islands, such a dispatch problem will be executed in each island for ensuring generation-load balance for each island. The objective (17) is to achieve the minimum operation costs, including costs of electricity generations and load shedding.

$$\min \sum_{j \in S_{\mathrm{EG}}} g_j(t)PG_j(t) + \sum_{i \in S_{\mathrm{ED}}} s_i(t)(D_i^0 - D_i(t)) \tag{17}$$

where $g_j(t)$ and $s_i(t)$ are cost coefficients for electricity generations and electricity demand shedding; S_{EG} and S_{ED} are the sets of electricity generators and electricity loads excluding natural gas compressors; D_i^0 is the initial electricity load at node i; $PG_j(t)$ is the dispatching variables of electricity generation and $D_i(t)$ is the remaining load after dispatching at time t. The value of $s_i(t)$ is chosen to be much larger than $g_j(t)$, aiming to unify the two objectives into a single optimization mode while considering load shedding as the last resort at different stages of the cascading failure propagation process.

The supply and demand balance of electricity power should be satisfied as

$$\sum_{j \in S_{\mathrm{EG}}} PG_j(t) = \sum_{i \in S_{\mathrm{ED}}} D_i(t) \tag{18}$$

Binary parameter $BI_b(t)$ is introduced to describe the status of electricity branch b. That is, $BI_b(t) = 0$ means electricity branch b is on outage during the cascading failure propagation process; otherwise$BI_b(t) = 1$.

DC power flow $F_b(t)$ through electricity branch b is modeled as in (19) and (20).

$$F_b(t) - \frac{\Delta\theta_b(t)}{x_b} - (1 - BI_b(t))L \leqslant 0 \tag{19}$$

$$F_b(t) - \frac{\Delta\theta_b(t)}{x_b} + (1 - BI_b(t))L \geqslant 0 \tag{20}$$

In (19) and (20), L is the "big M" value, x_b is the reactance of electricity branch b. When$BI_b(t) = 1$, (19) and (20) can be combined to derive the equality constraint, i.e., traditional power flow constraint through line; when$BI_b(t) = 0$, the value of L is chosen large enough to ensure that (19) and (20) are satisfied regardless of the voltage phase angle difference $\Delta\theta_b(t)$ of the two buses for branch b.

The remaining electricity load $D_i(t)$ after dispatching should satisfy the constraint

$$0 \leqslant D_i(t) \leqslant D_i^0 \tag{21}$$

The electricity generation $PG_j(t)$ is limited by its operation constraints

$$GI_j(t) \cdot PG_j^{\min} \leqslant PG_j(t) \leqslant GI_j(t) \cdot PG_j^{\max} \tag{22}$$

Power flow $F_b(t)$ through electricity branch b is subject to thermal limits of transmission capacity.

$$-BI_b(t)\cdot F_b^{\max} \leqslant F_b(t) \leqslant BI_b(t)\cdot F_b^{\max} \quad (23)$$

Voltage phase angle θ at electricity node i is also constrained by its upper and lower limits.

$$\theta_i^{\min} \leqslant \theta_i(t) \leqslant \theta_i^{\max} \quad (24)$$

Considering ramp up/down rates, the following constraints are imposed.

$$PG_j(t) - PG_j(t-1) \leqslant R_j^{+}\cdot GI_j(t) \quad (25)$$

$$PG_j(t-1) - PG_j(t) \leqslant R_j^{-}\cdot GI_j(t) \quad (26)$$

where R_n^+ and R_n^- are ramp up and ramp down limits of generator j.

2.5 Cascading failure evaluation indexes

Considering an IEGS operated at a steady state with initial gas demand M_n^0 at node n and electricity load D_i^0 at node i. At time t_{ini}, an initial failure arises either in gas or electricity sub-system, which will break the above mentioned initial steady state and could trigger the failure of other equipment in the IEGS successively. Finally, the IEGS could reach a new steady state with gas and electricity load $M_n(t_{\text{end}})$ and $D_i(t_{\text{end}})$ at the time t_{end}. The evolution process of IEGS from t_{ini} to t_{end} is called a cascading failure process.

Since the IEGS serves as a supplier to provide two types of energy, i.e. natural gas and electricity, to customers, comparing the availability of electricity and gas energy supply at the two steady-states respectively at the time instants t_{ini} and t_{end} before and after the cascading failure can analyze the impact of cascading failures on the energy service reliability of IEGS.

The impacts of cascading failure on electricity and natural gas service reliability are evaluated by the two indices of power load shedding $LOSS_{\text{p}}$ and gas load shedding $LOSS_{\text{g}}$, caused by a triggering event in a failure set. The two indexes are calculated by

$$LOSS_{\text{p}} = \sum_{i \in S_{\text{ED}}} D_i^0 - \sum_{i \in S_{\text{ED}}} D_i(t_{\text{end}}) \quad (27)$$

$$LOSS_g = \sum_{n \in S_{\text{GD}}} M_n^0 - \sum_{n \in S_{\text{GD}}} M_n(t_{\text{end}}) \quad (28)$$

where $D_i(t_{\text{end}})$ is the remaining power load at node i when the failure propagation ends, $M_n(t_{\text{end}})$ is the mass flow rate at node n at the new steady-state after the cascading failure. It is noteworthy that the evaluation index $LOSS_{\text{p}}$ could be negative, as a result of the increase in electricity consumptions of compressors. Similarly, the negative value of $LOSS_g$ indicates the rise of mass flow rates at gas-fired generator nodes.

2.6 Procedure of failure propagation simulation and evaluation

In order to evaluate the consequence of cascading failure propagation in IEGS statistically, a large number of failure event simulations is implemented, trigger by initial failures randomly chosen from the outage sets of gas pipelines and electricity branches. The integrated co-simulation procedure for describing and evaluating the cascading failure propagation in IEGS is illustrated as follows:

Step 1) Establish the initial failure sets of electricity branches and gas pipelines, and pre-define the number of simulation implementation.
Step 2) At $t = 0$, determine the initial steady-state in IEGS. With the values of electricity loads, gas demands, and gas source pressures, calculate the initial steady-state of gas network by steady-state model [40] and optimize the initial electricity generations according to (17)-(26).
Step 3) A failure propagation is initiated by choosing a triggering event from the pre-defined failures set.
Step 4) Implement electricity dispatch (17)-(26) to derive optimal electricity generation and load shedding, achieving a new electricity steady-state.
Step 5) Obtain the natural gas mass flow rates to gas-fired generators via (1) and the on/off states of compressors.
Step 6) Perform natural gas dispatching considering dynamic gas flow over the following ΔT time period (Strategy I in (6)-(12) or Strategy II in (6)-(10), (13)-(16)), where the appropriate operation mode switching of compressors, gas node pressure, and gas load shedding are determined.
Step 7) Derive electricity power consumptions of compressors via (2). If a generation gas load is shed, its corresponding power generation is set to zero.
Step 8) Set $t = t + \Delta T/\Delta t$ and go to *Step 4)* if the cascading failure still keeps propagating, utill operational values remain unchanged; otherwise, calculate cascading failure evaluation indexes by (27)-(28) and go to *Step 9)*.
Step 9) Go to *Step 3)* to initiate a new initial failure event if the number of simulation implementation is not reached; otherwise, the simulation procedure ends.

3. Simulation results

In this work, an IEGS shown in Figs. 2 and 3 is established to assess the cascading failure propagation process, which is composed of a 24-bus 35-branch electricity sub-system and a 29-node 26-branch natural gas sub-system. In the IEGS, the electricity and natural gas sub-systems are coupled by 3 gas-fired generators GG1-GG3 and 2 electricity-driven natural gas compressors CS1-CS2. Besides GG1-GG3, the electricity sub-system also includes 5 diesel generators denoted by DG1-DG5. GG1-GG3 also act as gas loads at nodes 16, 19, and 29 of natural gas network. In natural gas sub-system, two gas compressors denoted by CS1 and CS2 are respectively installed between nodes 11 and 17 as well as between nodes 27 and 6, which are supplied with electricity power at buses 13 and 15 of the electricity network. In natural gas network, three gas sources are installed at nodes 1, 12, and 21. In electricity network, the upper limit of active power flow through each branch is set as 130 MW, the upper limit of power output of each generator is set as 86 MW. For the compressors, the compress ratio, mass flow rate, and outlet pressure are constrained by [1.1, 1.9], [0 kg/s, 600 kg/s], and [1.0 MPa, 8.2 MPa]. The upper and lower limits of pressures at each gas load node are set as 1.3 and 0.7 times of its initial values. The

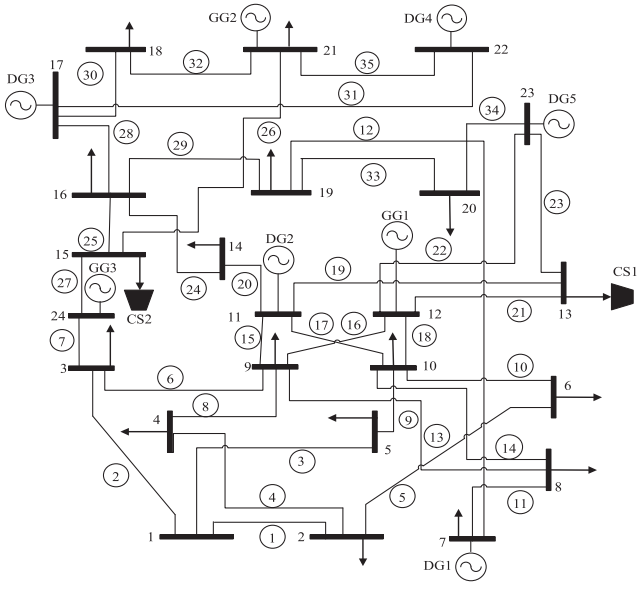

Fig. 2. Electricity network in IEGS.

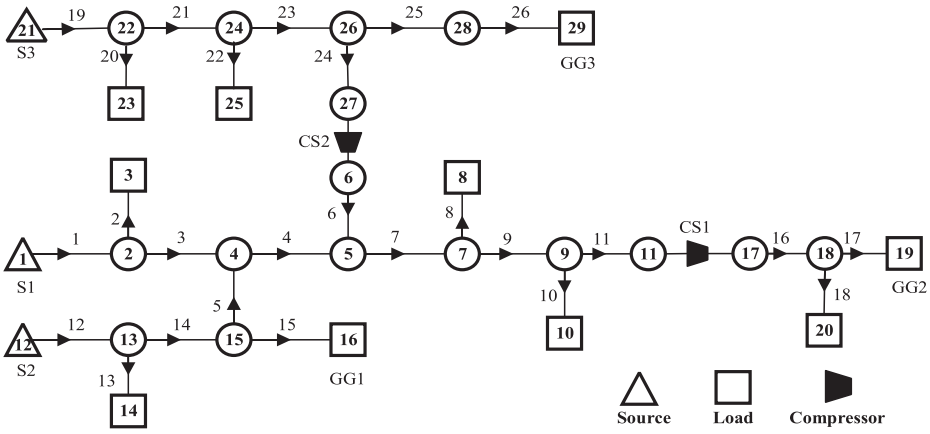

Fig. 3. Natural gas network in IEGS.

simulation parameters are set as $\Delta T = 8$ s and $\Delta t = 2$ s.

3.1 Cascading failure simulation and evaluation index

In electricity sub-system, since transmission lines are more susceptible to failure than buses and electricity transmission *N-k* contingencies has been widely used as a reliability standard, transmission *N*-3 outages are used as the failure set FS_p of electricity system. As for the failure set FS_g of natural gas sub-system, pipeline *N*-1 outages are considered, some of which can lead to the relatively severe consequence by the loss of gas source, for example pipelines 1, 12, 19, 21, 23 and so on. The outages of pipelines 6, 11, 16, and 24 directly connecting with gas compressors are not included in FS_g, assuming enough protection is given to them because of their higher importance.

Considering that the IEGS operates at a steady state initially, and at a certain time a failure is randomly chosen from the failure set FS_p or FS_g to trigger the cascading failure. Three different electricity load levels are studied:

Case 1) Normal load level, at which the initial steady-state operation status of electricity and gas variables in IEGS are given in Table 1;
Case 2) Peak load where electricity demand increases by 20% compared with Case 1;
Case 3) Valley load where electricity demand reduces by 20% compared with Case 1;

After the cascading failure propagates through the two systems, the IEGS can reach a new steady-state. For each failure in FS_p and FS_g, its cascading failure evaluation indexes are calculated according to equations (27) and (28) by comparing the new steady-state and the initial one. It should be noted that the simulation results given in Section III-A and III-B are derived using gas dispatching Strategy I because Strategy II has little effect in improving gas network reliability due to the slower dynamical process, which is illustrated in Section III-C. Take the peak load level in Case 2 as an example and list the evaluation indexes for several typical failures in FS_p and FS_g in Table 2. Among the failures in FS_p, electricity transmission *N*-3 contingency of branches [19,21,23] would cause the relatively more severe loss of electricity and natural gas supplies. The energy supplies losses resulting from the outages of gas branches 7, 9 and 19 are among the most severe ones in FS_g. Moreover, Table 2 also shows that the damages caused by gas branch failures are more serious than by electricity transmission *N*-3 contingencies. To this end, the operators should pay special attentions to the prevention of gas branch failures that would lead to relatively more severe losses to IEGS.

As shown in Table 2, failure of gas pipeline 7 would impose the most

Table 1
Initial steady-state operation values in IEGS in Case 1.

Pressures at nodes (MPa)						Mass flow rates of pipelines (kg/s)					
1	3.100	11	2.529	21	2.800	1	102.164	10	30.000	19	200.636
2	3.041	12	3.063	22	2.540	2	30.000	11	121.722	20	30.000
3	3.036	13	3.027	23	2.534	3	72.164	12	80.000	21	170.636
4	3.012	14	3.021	24	2.334	4	81.722	13	30.000	22	30.000
5	2.973	15	3.012	25	2.327	5	9.557	14	50.000	23	140.636
6	3.030	16	3.003	26	2.182	6	100.000	15	40.443	24	100.000
7	2.775	17	3.800	27	2.1020	7	181.722	16	121.722	25	40.636
8	2.770	18	3.732	28	2.169	8	30.000	17	41.722	26	40.636
9	2.628	19	3.724	29	2.156	9	151.722	18	80.000		
10	2.622	20	3.702								
Power flows through branches (MW)						Net injection power at buses (MW)					
1	29.076	13	9.932	25	60.112	1	0	9	−19.845	17	74.449
2	−26.431	14	21.634	26	−51.608	2	−38.930	10	−27.860	18	–33.965
3	−2.645	15	−16.613	27	−18.373	3	–22.135	11	72.620	19	–23.280
4	−9.579	16	−27.029	28	−87.803	4	−29.770	12	72.210	20	−51.525
5	−0.280	17	−41.160	29	7.050	5	−28.625	13	−10.110	21	24.495
6	5.616	18	−51.575	30	15.949	6	−54.960	14	−77.860	22	74.433
7	−54.182	19	−12.223	31	−29.304	7	73.141	15	−9.870	23	73.606
8	−39.345	20	27.070	32	−18.016	8	−18.700	16	−90.075	24	72.556
9	−31.270	21	5.704	33	6.646						
10	−55.240	22	−12.098	34	−44.879						
11	50.266	23	−16.629	35	−45.129						
12	22.876	24	−50.790								

Table 2
Cascading failure evaluation indexes in Case 2.

N-3 electric line outages	N-1 gas pipeline outages	$LOSS_p$ (MW)	$LOSS_g$ (kg/s)
[19,21,23]	–	86.2524	128.1790
[7,26,27]	–	118.6906	54.3713
[7,30,32]	–	33.7202	12.2109
[25,26,27]	–	33.0082	6.4110
[1,6,34]	–	0.0040	0.0118
–	Branch 7	90.3914	188.8620
–	Branch 9	89.7673	158.6520
–	Branch 19	109.5039	111.9791
–	Branch 4	2.9364	60.6233
–	Branch 17	91.5610	49.0644
–	Branch 23	88.4362	48.5417
–	Branch 26	86.7245	48.2625
–	Branch 25	86.0290	48.1496
–	Branch 15	85.7966	48.1083
–	Branch 21	33.0624	37.1628
–	Branch 5	0.0578	0.0124
–	Branch 14	−0.0586	−0.0111
–	Branch 3	−0.1166	−0.0227
–	Branch 12	−0.1364	−0.0267
–	Branch 1	−0.1683	−0.0330

serious impact on IEGS in terms of the loss of gas and electricity energy supplies. The cascading failure propagation process induced by this contingency is described as follows. When outage of pipeline 7 occurs at $t = 400$ s, the gas network is divided into two isolated islands with no gas source on the right island. Then, pressures at nearby nodes 7–11 drop rapidly, and compress ratio of CS1 increases sharply and quickly reaches the upper limit at $t = 440$ s, with its working mode switched from mode 1 to mode 2. Due to significant drop of pressure at nodes 8 and 10, gas loads at nodes 8 and10 are respectively shed at $t = 448$ s and $t = 464$ s. The lack of gas source on the right island leads to the removal of the other two gas loads at nodes 19 and 20 at $t = 544$ s, and gas-fired generator GG2 is forced off-line immediately. As a result, almost no gas mass flows through CS1 which makes its electric power consumption go down sharply, and power rescheduling leads to total 90.3914 MW electricity load shedding instantly after the outage of GG2.

In electricity network, we consider outages of branches 19, 21, and 23 occur at $t = 400$ s, which divide the electricity network into two isolated islands: bus 13 and the remaining system. Specifically, in the island including bus 13 only, there is no electricity supply to CS1, forcing it into mode 4 right after the initial outages. This leads to a significant drop of pressure at nodes 17 and 18, and gas loads at nodes 19 and 20 are shed at $t = 472$ s after a transient period. Gas load shedding at node 19 means the forced off-line of gas-fired generator GG2, and then the immediate dispatching in electricity network induces more electricity load shedding, reaching 86.2524 MW. In the natural gas network, removal of gas loads at nodes 19 and 20 leads to total 128.1790 kg/s gas load shedding.

In Table 2, failures of certain gas pipelines, such as 1, 3, 12, and 14, could lead to negative $LOSS_p$ and $LOSS_g$. We take pipeline 1 as an example to illustrate. The outage of pipeline 1 will triggers the increase in compress ratio of CS1 and decreases compress ratio of CS2, which impacts their corresponding power consumptions. The total power consumption by the two compressors increases, and with the power increase of all generators with no electricity load shedding occurs. Negative $LOSS_p$ and $LOSS_g$ result from the increased electricity demands from compressors and the increased gas demands from gas-fired generators. Although the outage of pipeline 1 brings about the direct loss of gas source 1 which supplies 23.74% of total gas loads, there is no damage to the IEGS owing to the flexible operation capabilities of compressors.

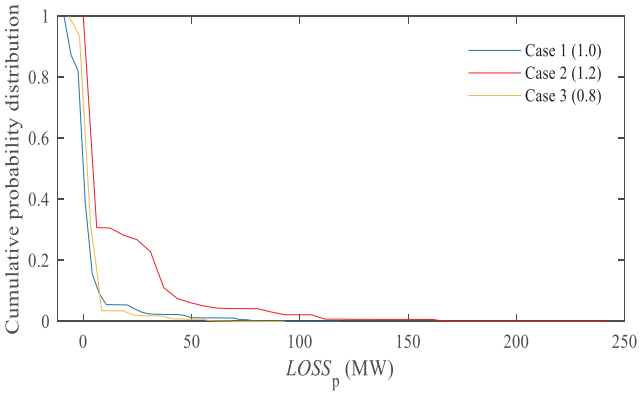

Fig. 4. Cumulative probability distribution of $LOSS_p$ under failures in FS_p.

3.2 Statistical analysis on interactive influence of cascading propagation

Interactive influence of the cascading failure propagation initialized in one sub-system on another is analyzed statistically by randomly choosing a contingency from the failure set FS_p 10,000 times and from the failure set FS_g 1000 times, and then calculating the statistical results of evaluation indexes. The different numbers of simulations for the two failure sets mainly consider the fact that the number of outages in FS_p is much larger than that in FS_g. For the initial steady states in Cases 1–3, the power generation from gas-fired generators respectively accounts for 37.32%, 37.50%, and 37.09% of total generation, the electricity loads of compressors occupy 3.4%, 3.25%, and 3.72% of total electricity loads, the gas demands from gas-fired generators occupy 32.08%, 35.71%, 27.37% of total gas demands.

The cumulative probability distributions of cascading failure evaluation indexes, triggered by the outages in FS_p, are depicted in Figs. 4 and 5. As shown in Fig. 4, at low and normal electric load levels, the risks of power load shedding are relatively negligible. With the increase in power load level, the cumulative probability of power load shedding rises significantly, but it is still not severe; the probability of over 50 MW electricity load shedding (i.e., about 8.51% of total electric demand) is only about 6.1%, and that of over 200 MW shedding is close to 0.

Fig. 5 indicates that, at three electric load levels, the risks of gas load shedding caused by electricity contingencies are almost negligible, much lower than the risks of power load shedding. From the cascading failure simulations, it is shown that the gas load shedding induced by electricity contingency mainly comes from the outages of gas-fired generators and compressors, which are usually the results of electricity island. The former leads to the direct loss of gas loads, and the latter brings about the gas pressure drop and the possible loss of other generation or non-generation gas loads after a transient period. Fig. 5

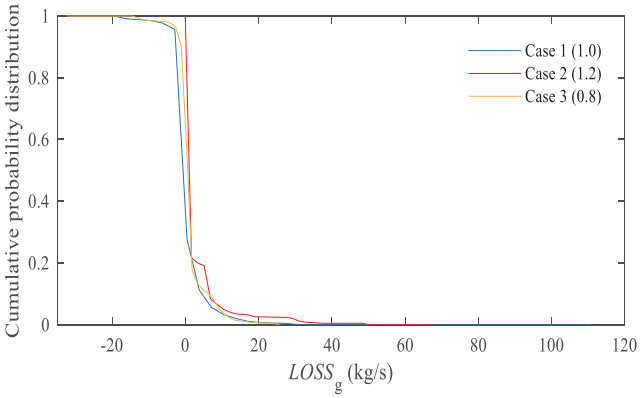

Fig. 5. Cumulative probability distribution of $LOSS_g$ under failures in FS_p.

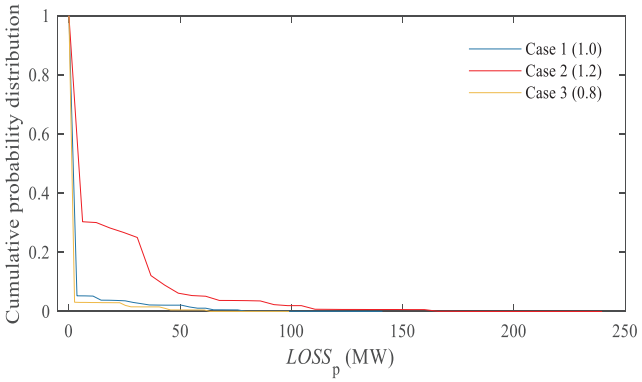

Fig. 6. Cumulative probability distribution of $LOSS_p$ under failures in FS_p without gas-fired generators.

reveals that the probabilities of compressor and gas-fired generator failures caused by contingencies in FS_p are very low, and negligible impact is imposed on gas network operation. It can be explained by the following reasons: the smaller proportion of compressor electricity consumption in total electricity demand, and the robustness of natural gas system against the failure spreading from electricity network owing to the flexible gas linepack and elastic compressor operation modes.

In order to further examine the impact of natural gas network on cascading failure propagation triggered by electricity contingencies, a comparison is implemented by replacing the three gas-fired generators GG1-GG3 with diesel generators. The corresponding cumulative probability distributeon of $LOSS_p$ under failures in FS_p is depicted in Fig. 6, which is almost identical to Fig. 4. The phenomenon indicates that the triggering contingency from electricity network may not propagate into the gas network, and in turn the limited risk of gas load shedding.

The cumulative probability distributions of cascading failure evaluation indexes, triggered by the contingencies in FS_g, are drawn in Figs. 7 and 8. At peak load level, the probability of medium- and small-scale power load shedding (<110 MW) is very high; on the contrary, the probability of large-scale power load shedding is zero. At normal and low load levels, the power load shedding risk becomes lower, but still higher than the corresponding ones in Fig. 4, especially for the smaller-scale load shedding. The outages initialized in gas network have influence on the power gird mainly by the varying electricity consumptions of compressors and electricity generations of gas-fired generators. Owing to the relatively small proportion of compressors' electricity consumptions in the total demand and the relatively sufficient reserve capacity, the consequences caused by the failures in FS_g are insignificant when the electricity network operates at normal and low load levels. In comparison, at high load level, the risk of medium- and small-scale power load shedding caused by the contingency in FS_g is much more severe than that induced by the contingency in FS_p. The reason

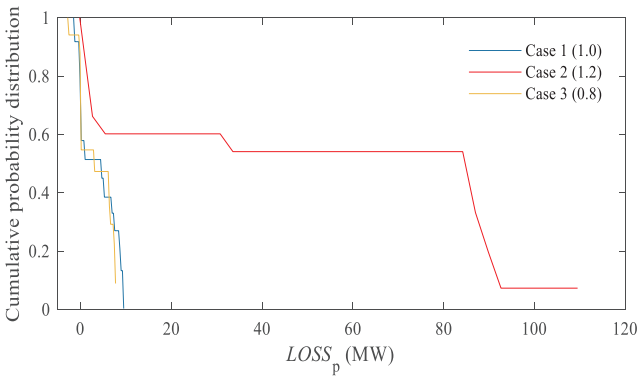

Fig. 7. Cumulative probability distribution of $LOSS_p$ under failures in FS_g.

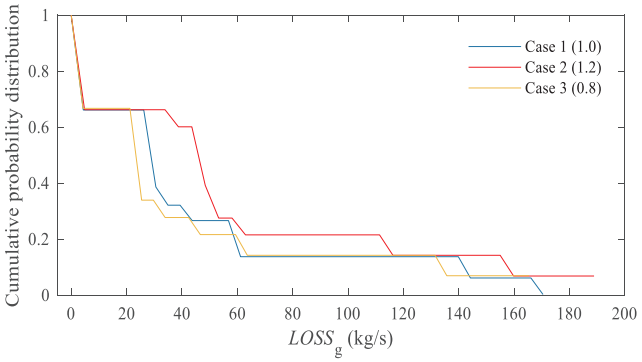

Fig. 8. Cumulative probability distribution of $LOSS_g$ under failures in FS_g.

can be illustrated as follows. From the natural gas network topology, it is discovered that the failures of a number of pipelines can lead to the loss of gas source 3 which offers about 51% of total gas demand as well as the outage of gas-fired generator. These failures are different from those propagated from electricity network to gas network. The former are direct and destructive; however, the latter are indirect and mild. The significant difference can also be clearly observed by comparing Figs. 5 and 8. The destructive failures directly imposed on the gas network, along with the higher proportion of gas-fired generation in total generation and the insufficient reserve capacity at high load level, can lead to more severe risk of medium- and small-scale power load shedding.

As shown in Fig. 8, the cumulative probabilities of gas load shedding are similar at different electric load levels. This phenomenon can be illustrated as follows. Electricity dispatching induced by the outages in gas network is less likely to bring about the loss of other gas-fired generators and the off-line of compressors. Even if the power supply outages to compressors may occur, no further gas load shedding arises owing to the flexibility of gas system.

For the gas network contingencies as the triggering events, a new study is implemented to observe the influence of gas-fired generators on the cascading failure propagation. In this study, only gas-fired generator GG2 is kept, while GG1 and GG3 are replaced by diesel generators and these two generation gas demands replaced by non-generation demands in gas network. The corresponding cumulative probability distribution of $LOSS_p$ under failures in FS_g is depicted in Fig. 9. As shown in Fig. 9, at normal and low load levels, the power load shedding risk is almost identical to that in Fig. 7; however, at peak load level, the power load shedding risks are much lower than those in Fig. 7. This phenomenon indicates that in IEGS under gas pipeline contingencies, the power system reserve capacity is the most critical factor in supplying reliable generation, while the coupling of gas-fired generators is the second most critical factor.

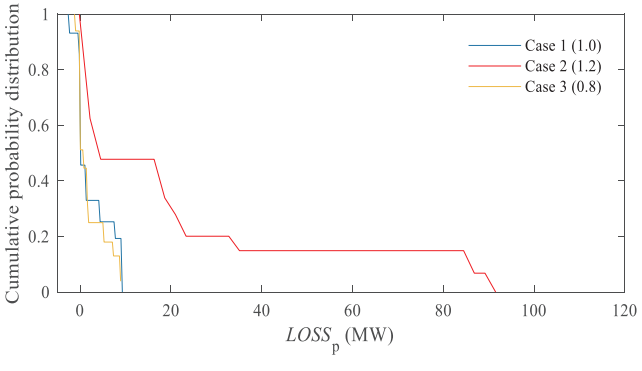

Fig. 9. Cumulative probability distribution of $LOSS_p$ under failures in FS_g with only one gas-fired generator GG2.

3.3 Discussions

Remark 1: In the natural gas network, dispatching strategy of adjusting gas source pressures at a shorter timescale under contingencies could present limited effect in improving the reliability. This can be illustrated from the following two aspects:

On one hand, as shown in Fig. 4, the natural gas network is usually connected in a radial topology, which cannot provide strong flexibility of gas supply as compared to the networked topology. For example, the outage of pipeline 7 may cut off the gas supply to its downstream gas loads at nodes 8, 10, 19, and 20. Similarly, outages of pipelines 19, 21, and 23 could also cause the sharp drop of their downstream pressures and induce gas loads shedding.

On the other hand, in the gas network, pipeline 5 as well as the connection between nodes 26 and 5 can offer an alternative gas supply channel when a gas source outage occurs. Outage of gas pipeline 4 is taken as an example to show limited effect imposed by the dispatching Strategy II on improving the reliability of gas supply due to slower gas transmission dynamics. As shown in Fig. 4, before outage of gas pipeline 4, almost half of the gas demands at nodes 8, 10, 19, and 20 is supplied by gas source S1. After outage of pipeline 4, the gas transmission channel from gas source S1 to nodes 8, 10, 19, and 20 is broken, and we shall optimize gas source S3 at node 21 to maintain pressures at nodes 8, 10, 19, and 20 by applying gas dispatching Strategy II. Mass flow rates at demand nodes 8, 10, and 20, as well as pressures at gas demand nodes 8, 10, and 20 and gas source S3 are depicted in Figs. 10 and 11, respectively. As shown in Fig. 10, after outage of gas pipeline 4 occurs at $t = 400$ s, pressures at gas nodes 8 and 10 gradually drop, and dispatching Strategy II begins to adjust pressure of gas source S3 when nodal pressures violate the limits over the dispatching horizon. Although pressure at gas source S3 is lifted, it cannot immediately prevent pressures at demand nodes from falling due to slower dynamics. As a result, all gas demands at node 10 and partial gas demands at nodes 8 and 20 are still shed respectively at $t = 776$ s and $t = 880$ s, as depicted in Fig. 11. If gas dispatching Strategy I is implemented, all gas demands at nodes 8 and 10 are shed respectively at $t = 728$ s and $t = 776$ s, as a result of pressure constraints violations.

Remark 2: Dispatching in the electricity network under contingency could diminish the cascading influence on the coupled natural gas subsystem.

The main reason is that dispatching in the electricity network under contingency could help mitigate the effects of contingencies occurred in the electricity network, making the energy coupling components less involved and further imposing less impact on the coupled natural gas sub-system. Take the transmission N-3 contingency of the electricity network [25,28,32] as an example. When electricity branches 25, 28, and 32 encounter outages, if there is no electricity dispatching, the active power flows through branches 7, 26, and 27 will exceed their upper limits. As a result, the three branches are forced into outages. Thus, failures of branches 7, 25–28, and 32 divide the electricity network into four isolated islands, i.e. bus 15, bus 24, buses 17, 18, 21, 22, and the remaining system. In the island with bus 15, CS2 has no electricity supply, and is forced into mode 4. In the island with bus 24, only the gas-fired generator GG3 is left, so its output is cut to 0 MW, inducing 47.2677 kg/s gas load shedding in the gas network. On the contrary, if electricity dispatching is implemented after the occurrence of N-3 branch contingency [25,28,32], the influence of contingency can be mitigated by adjusting electric generation and demand, with only 1.0128 kg/s gas load shedding.

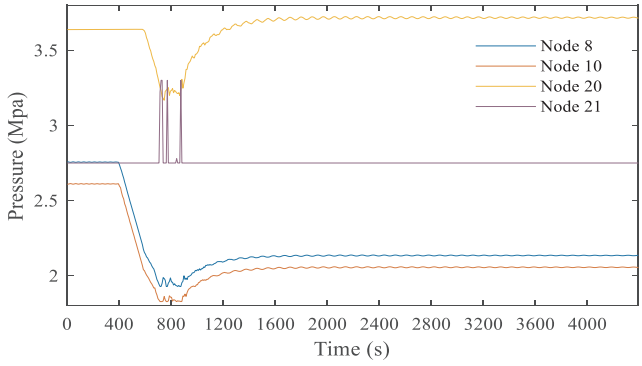

Fig. 10. Pressure at gas load nodes by adopting gas dispatching Strategy II after the occurrence of pipeline 4 outage.

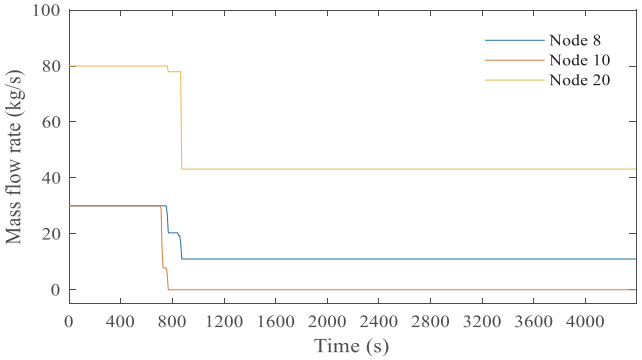

Fig. 11. Mass flow rates at gas load nodes by adopting gas dispatching Strategy II after the occurrence of pipeline 4 outage.

4. Conclusions

This study investigates and evaluates the cascading failure propagation in IEGS with energy coupling components, including gas-fired generators and electricity-driven gas compressors. An integrated simulation approach that combines dynamic gas transmission and steady-state power flow is proposed, while considering electricity islanding and dispatching of electricity generation and gas source pressure as well as electricity and gas load shedding. Evaluation indexes for assessing cascading failure consequence are developed, and the statistical results for indexes are derived by simulations. The proposed approach can describe the propagation process of cascading failure between the two subsystems. The outages in failure sets of electricity or natural gas system with disastrous consequence can be identified, which, if secured with high priority, could help prevent the potential catastrophe. The distinguished cascading effects of electricity and natural gas sub-systems on each other are revealed. Facing with the spreading of cascading failure within IEGS, natural gas system is more likely to propagate the failure to electricity system since its post-contingency dispatching has negligible effect because slower dynamics though flexible linepack and compressor working mode switching can help smooth local small disturbance; on the contrary, immediate effect of electricity dispatching can mitigate the cascading failure propagation from electricity system to gas system. The developed approach can help the energy system operators better understand the mechanism of cascading failure propagation in IEGS and suggest the appropriate prevention measures.

CRediT authorship contribution statement

Zhejing Bao: Methodology, Software, Writing - original draft. **Zhewei Jiang:** Methodology, Software, Validation, Writing - original draft. **Lei Wu:** Methodology, Writing - review & editing.

Declaration of Competing Interest

The authors declare that they have no known competing financial interests or personal relationships that could have appeared to

influence the work reported in this paper.

Acknowledgment

This work was supported by the National Natural Science Foundation of China under Grant no. 51777182, and in part supported by the U.S. National Science Foundation under Grant no. CMMI-1635339.

References

[1] Omalley M, Kroposki B. Energy comes together: the integration of all systems. IEEE Power Energy Mag 2013;11(5):18–23.
[2] Mancarella P. MES (multi-energy systems): an overview of concepts and evaluation models. Energy 2014;65:1–17.
[3] Moein M, Ali A, Mahmud F, Ehsan H. A decomposed solution to multiple-energy carriers optimal power flow. IEEE Trans Power Syst. 2014;29(2):707–16.
[4] Ding T, Xu Y, Wu L, Wei W. Energy flow optimization for integrated power-gas generation and transmission systems. IEEE Trans Ind Inform 2019. https://doi.org/10.1109/TII.2019.2924927.
[5] Wang C, Wei W, Wang J, Wu L. Equilibrium of interdependent gas and electricity markets with marginal price based bilateral energy trading. IEEE Trans Power Syst Sep. 2018;33(5):4854–67.
[6] Zlotnik A, Rudkevich A, Carter R, Ruiz P, Backhaus S, Taft J. Grid architecture at the gas-electric interface. Technical Report, Grid modernization laboratory consortium; Jun. 2017.
[7] Chen S, Conejo A, Sioshansi R, Wei Z. Equilibria in electricity and natural gas markets with strategic offers and bids. IEEE Trans Power Syst 2019. https://doi.org/10.1109/TPWRS.2019.2947646.
[8] Zhao B, Zlotnik A, Conejo A, Sioshansi R, Rudkevich A. Shadow price-based co-ordination of natural gas and electric power systems. IEEE Trans Power Syst 2019;34(3):1942–54.
[9] Carlos M, Pedro S. Integrated power and natural gas model for energy adequacy in short-term operation. IEEE Trans Power Syst 2015;30(6):3347–55.
[10] Shahidehpour M, Fu Y, Wiedman T. Impact of natural gas infrastructure on electric power systems. Proc IEEE 2005;93(5):1042–56.
[11] Levitan R, Wilmer S, Carlson R. Unraveling gas and electric interdependencies across the eastern interconnection. IEEE Power Energy Mag 2014;12(6): 78–88.
[12] Hibbard P, Schatzki T. The interdependence of electricity and natural gas: current factors and future prospects. Electr J 2012;25(4):6–17.
[13] Judson N. Interdependence of the electricity generation system and the natural gas system and implications for energy security. Technical Report 1173; May 2013.
[14] Li T, Eremia M, Shahidehpour M. Interdependency of natural gas network and power system security. IEEE Trans Power Syst 2008;23(4):1817–24.
[15] Munoz J, Jimenez-Redondo N, Perez-Ruiz J, Barquin J. Natural gas network modeling for power systems reliability studies. Proc IEEE Bologna Power Tech Conf 2003;4:1–8.
[16] Liu C, Shahidehpour M, Fu Y, Li Z. Security-constrained unit commitment with natural gas transmission constraints. IEEE Trans Power Syst 2009;24(10):1523–35.
[17] Erdener B, Pambour K, Bolado-Lavin R, Dengiz B. An integrated simulation model for analysing electricity and gas systems. Electr Power Energy Syst, 2014;61:410–20.
[18] Pambour K, Erdener B, Bolado-Lavin R, Dijkema G. SAInt-A novel quasi-dynamic model for assessing security of supply in coupled gas and electricity transmission networks. Appl Energy 2017;203:829–57.
[19] Pambour K, Erdener B, Bolado-Lavin R, Dijkema G. Development of a simulation framework for analyzing security of supply in integrated gas and electric power systems. Appl Sci 2017;7(47):1–32.
[20] Chen S, Wei Z, Sun G, Wang D, Zang H. Steady state and transient simulation for electricity-gas integrated energy systems by using convex optimization. IET Gener Transm Distrib 2018;12(9):2199–206.
[21] Qiao Z, Guo Q, Sun H, Pan Z, Liu Y, Xiong W. An interval gas flow analysis in natural gas and electricity coupled networks considering the uncertainty of wind power. Appl Energy 2017;201:343–53.
[22] Zhao B, Conejo A, Sioshansi R. Unit commitment under gas-supply uncertainty and gas-price variability. IEEE Trans Power Syst 2017;32(3):2394–405.
[23] Diagoupis T, Andrianesis P, Dialynas E. A planning approach for reducing the impact of natural gas network on electricity markets. Appl Energy 2016;175:189–98.
[24] Zhao B, Conejo A, Sioshansi R. Coordinated expansion planning of natural gas and electric power systems. IEEE Trans Power Syst 2018;33(3):3064–75.
[25] He C, Wu L, Liu T, Wei W, Wang C. Co-optimization scheduling of interdependent power and gas systems with electricity and gas uncertainties. Energy 2018;159:1003–15.
[26] He C, Wu L, Liu T, Bie Z. Robust co-optimization planning of interdependent electricity and natural gas systems with a joint N–1 and probabilistic reliability criterion. IEEE Trans Power Syst 2018;33(2):2140–54.
[27] Corra-Posada C, Sánchez-Martın P. Security-constrained optimal power and natural-gas flow. IEEE Trans Power Syst. 2014;29(4):1780–7.
[28] Chen S, Wei Z, Sun G, Cheung K, Sun Y. Multi-linear probabilistic energy flow analysis of integrated electrical and natural-gas systems. IEEE Trans Power Syst 2017;32(3):1970–9.
[29] Clegg S, Mancanrella P. Integrated modeling and assessment of the operational impact of power-to gas (P2G) on electrical and gas transmission networks. IEEE Trans Sustain Energy 2015;6(4):1234–44.
[30] Martínez-Mares A, Fuerte-Esquivel C, Ingeniería I. Integrated energy flow analysis in natural gas and electricity coupled systems. In: 2011 North American power symposium; Aug. 2011. p. 1–7.
[31] Liu C, Shahidehpour M, Wang J. Coordinated scheduling of electricity and natural gas infrastructures with a transient model for natural gas flow. Chaos 2011;21.
[32] Wang C, Wei W, Wang J, Liu E, Qiu F, Cerrea-Posada C, et al. Robust defense strategy for gas-electric systems against malicious attacks. IEEE Trans Power Syst 2017;32(4):2953–65.
[33] Alabdulwahab A, Abusorrah A, Zhang X, Shahidehpour M. Stochastic security-constrained scheduling of coordinated electricity and natural gas infrastructures. IEEE Syst J 2017;11(3):1674–83.
[34] He C, Dai C, Wu L, Liu T. Robust network hardening strategy for enhancing resilience of integrated electricity and natural gas distribution systems against natural disasters. IEEE Trans Power Syst 2018;33(5):5787–98.
[35] He C, Zhang X, Liu T, Wu L. Distributionally robust scheduling of integrated gas-electricity systems with demand response. IEEE Trans Power Syst 2019. https://doi.org/10.1109/TPWRS.2019.2907170.
[36] Fu X, Zhang X. Failure probability estimation of gas supply using the central moment method in an integrated energy system. Appl Energy 2018;219:1–10.
[37] Fu X, Zhang X, Qiao Z, Li G. Estimating the failure probability in an integrated energy system considering correlations among failure patterns. Energy 2019;178:656–66.
[38] Shen Y, Gu C, Zhao P. Structural vulnerability assessment of multi-energy system using a PageRank algorithm. In: 10th International conference on applied energy (ICAE2018); Aug. 2018, Hong Kong, China.
[39] Fang J, Zeng Q, Ai X, Chen Z, Wen J. Dynamic optimal energy flow in the integrated natural gas and electrical power systems. IEEE Trans Sustain Energy 2018;9(1):188–98.
[40] Bao Z, Chen D, Wu L, Guo X. Optimal inter- and intra-hour scheduling of islanded integrated-energy system considering linepack of gas pipelines. Energy 2019;171(1):326–40.